

Graphene Oxide Epoxy Resin for Improving Anticorrosive Properties

Nurul Anis Athirah Ab Aziz, Chin Wei Lai*, and Boon Hoong Ong

Nanotechnology & Catalysis Research Centre, Institute for Advanced Studies, University of Malaya, 50603 Kuala Lumpur, Malaysia.

*Corresponding author. e-mail: cwlai@um.edu.my

ABSTRACT

In this study, anticorrosive coatings were developed for mild steel surfaces using epoxy resin as a barrier with a high aspect ratio. The study investigated the impact of modifying graphene oxide (GO) with d-glucose (D-g) on protecting mild steel from corrosion in a 3.5 wt.% sodium chloride (NaCl) solution for 42 days. The hydrophilic nature of D-glucose, GO, and EP enabled the formation of nanocomposites with uniform distribution of D-g-modified GO in the EP coatings, reducing free volume in the epoxy matrix. The 0.7% D-g modified GO/EP coating exhibited strong anticorrosion properties even in highly corrosive conditions by achieving a high corrosion resistance value of -19.405 mm/year. According to the morphological observation, the 0.7% m-GO/EP coating displayed fewer invisible rusts on the metal substrate even after 42 days. Incorporating D-g/GO significantly improved the corrosion protection performance of the coatings by combining EP and graphene. This study marks the first report on D-g modified GO/EP composite coatings for enhanced anticorrosive properties, making it a noteworthy contribution to eco-friendly corrosion protection mechanisms in EP coating systems in Malaysia. The environmentally friendly approach aligns with sustainable development principles and has garnered global attention from researchers and scientists. Earlier research has extensively explored the effect of surface-functionalized GO particles on the corrosion resistance of polymeric coatings.

Keywords: Anticorrosion, d-glucose, epoxy coating, modified graphene oxide, steel

1. INTRODUCTION

Due to rapid technological and scientific advancements, the study of corrosion phenomena has recently gained significant attention. Metal corrosion is common in industrial settings, leading to substantial financial losses and compromising equipment reliability. Corrosion, an inevitable electrochemical/chemical process, adversely affects the desirable qualities of metals. The active surfaces of these materials interact with the environment, resulting in aggressive corrosion [1]. In general, there are two approaches to preventing corrosion: active and passive strategies, which aim to delay the progression of corrosion activities [2], [3]. A growing trend in the literature shows an increased interest in the use of anticorrosive coatings that incorporate nanoparticles into polymer matrices [4].

Polymer coatings are commonly used to minimize corrosion on steel substrates. These coatings incorporate various organic compounds and offer excellent anticorrosion properties [5]–[9]. Among the different types of polymers, epoxy is highly valued for its durability, resilience, and ability to protect against heat and chemical damage [10]–[12]. However, despite its advantageous characteristics, epoxy resins have limitations in terms of outdoor endurance [13], [14]. To address this concern, epoxy hybrids are widely employed in various industries. The existence of micro-voids in the polymers can lead to hydrophilicity, resulting in coating degradation [15], [16].

These pores also allow corrosive ions to penetrate the coating-metal interface. Numerous studies have been conducted to enhance the properties of polymers to overcome these challenges [17], [18].

In recent years, carbon-based nanoparticles, particularly graphene oxide (GO), have gained considerable interest as additives for organic coatings due to their exceptional mechanical properties and distinctive attributes [19], [20]. GO's appealing features, including excellent thermal stability, a large specific surface area, and moisture impermeability, coupled with abundant polar functional groups in its structure, make it a desirable option. Incorporating GO into organic coatings significantly enhances their overall mechanical strength and durability. Additionally, GO's compatibility with various organic matrices improves adhesion, making coatings more resistant to wear, temperature fluctuations, and moisture. It is an innovative and promising choice for researchers and industries exploring advanced coating applications [21]–[23].

Graphene, consisting of hexagonally arranged carbon atoms in a two-dimensional structure, possesses remarkable properties such as thermal and electrical conductivity, chemical and thermal stability, high mechanical strength, and impermeability [24], [25]. These exceptional qualities make graphene an ideal candidate for barrier materials in anti-corrosive coatings. As a result, it has found widespread use in various industrial fields, including aerospace, electronics, and bioengineering. Graphene's successful application as a reinforcement in composite coatings has

been well documented, regardless of whether the matrix is ceramic, metallic, or polymer [26], [27]. Incorporating graphene into resins significantly improves the electrical and mechanical properties of polymeric mediums, leading to the development of multifunctional coatings [28], [29]. Graphene also protects the coated substrate and enables the creation of flame-retardant, anti-fouling, and wear-resistant layers.

Moreover, when added to polymeric matrices, graphene dramatically enhances the corrosion resistance of composite coatings by creating a tortuous path for aggressive species and uniformly distributing it in the polymer matrix, preventing accumulation [30]–[32]. However, graphene's distribution as a filler in the resin can be limited by agglomeration due to strong Van der Waals forces, and microscopic phase separation may occur during the cure time [33], [34]. Additionally, the increased viscosity of coatings with a higher percentage of graphene nanoparticles can pose challenges during application. Bahadur et al. presented experimental findings indicating that graphene oxide (GO) coatings demonstrated outstanding protection for metallic materials [35]–[37]. Functional groups like hydroxyl, carbonyl, carboxyl, and epoxy groups in GO provide active sites, enabling easy covalent and noncovalent functionalization. The functionalization enhances the dispersion and compatibility of GO nanosheets within the organic coating, further contributing to its performance [38], [39].

In this study, we developed anticorrosive coatings on the surface of mild steel using epoxy resin with a high aspect ratio as a barrier. The inspiration for this research came from a recent journal, which motivated our team to explore an efficient and eco-friendly approach by incorporating natural chemicals into GO/EP nanocomposite coatings to enhance their anticorrosive properties. We investigated the use of D-glucose (D-g) as a natural chemical to modify the surface of GO and evaluate its anticorrosion properties on the mild steel substrate by immersing it in a 3.5 wt.% sodium chloride (NaCl) solution for 42 days. Hydroxyl groups in D-glucose are expected to facilitate the crosslinking between epoxy and GO, leading to excellent anticorrosive properties. As D-glucose, GO, and EP are hydrophilic, we formed nanocomposites in situ using water as a dispersant solvent, ensuring uniform dispersion of D-g modified GO within EP coatings and reducing free volume in the epoxy matrix. Notably, no previous reports exist on D-g modified GO/EP composite coatings for improving anticorrosive properties, making our research a significant contribution to corrosion protection mechanisms using eco-friendly and natural-based chemicals in EP coating systems in Malaysia. The potential benefits of this environmentally friendly approach align with the principles of sustainable development, attracting global attention from researchers and scientists.

2. MATERIAL AND METHODS

2.1. Materials

The material of the coating adopts epoxy resin, and the coating substrate adopts mild steel. The steel substrates with measurements of 1.5 mm × 50 mm × 50 mm were used throughout this experiment for corrosion study. The basic materials used in this study are illustrated in Table 1. Distilled water is used throughout this study.

Table 1 Details about the chemicals used in this study

Chemical	Supplier	Mass purity
Sulfuric acid (H₂SO₄)	Merck	≥ 95-97 %
Phosphoric acid (H₃PO₄)	Sigma-Aldrich	85 %
Potassium permanganate (KMnO₄)	Friendemann Schmidt Chemical	≥ 99%
Hydrogen peroxide (H₂O₂)	Merck	≥ 30%
Hydrochloric acid (HCl)	Merck	≥ 37%
Ammonium hydroxide (NH₄OH)	Riedel-de Haen	25%
D-glucose (D-g)	Alfa Aesar	-

2.2 Synthesis of Graphene Oxide (GO)

The GO samples will be synthesized using the modified Hummers' method. Concentrated H₂SO₄/H₃PO₄ will be mixed in a 9:1 ratio. Firstly, 3g of graphite powder will be introduced and mixed for around 30 minutes. The mixture will then be carefully added 9g of KMnO₄ while being stirred in an ice bath with a temperature of less than 35 °C. The mixture is kept on a magnetic stirrer at room temperature for three days to ensure that the oxidation process is accomplished. Throughout the stirring phase, a dark brown colour will be achieved. After three days, a solution of distilled water and H₂O₂ will be progressively poured into the graphene mixture to stop the oxidation reaction. The light brown tint achieved indicates a significant degree of graphite oxidation. The GO will be centrifuged 3-4 times with HCl and distilled water before being cleansed with distilled water till pH 5 is obtained. The GO precipitation will be dried at 50 °C in a vacuum drying oven for a few hours.

2.3 Synthesis of Modified Graphene Oxide (m-GO)

At 90 °C, the GO suspension will be stirred for two hours with 0.1 g of D-g. The mixture will then be treated with NH₄OH to improve the pH to 9-10. The functionalized GO will next be centrifuged and rinsed three times with distilled water to eliminate any remaining D-g. After that, the mixture is sonicated for 90 minutes at 50 °C.

2.4 Synthesis of m-GO/EP

Modified GO powder (0.10-1.0 g) will be disseminated in distilled water with the ultrasonic process for 60 minutes at 40 °C. 4 g of EP will be added to a modified GO suspension and sonicated for 10 minutes. The remaining solvent will be removed by heating the mixture to 40 °C. Following that, 16 g of curing agent will be mixed into the mixture, agitated for around five minutes, then degassed for 10 minutes at 40 °C in a vacuum drying oven to eliminate air bubbles. Lastly, the modified GO/EP (m-GO/EP) will be applied on mild steel using the dip-coating approach. Furthermore, without GO, pure EP and solvent-based epoxy resin will be made for evaluation.

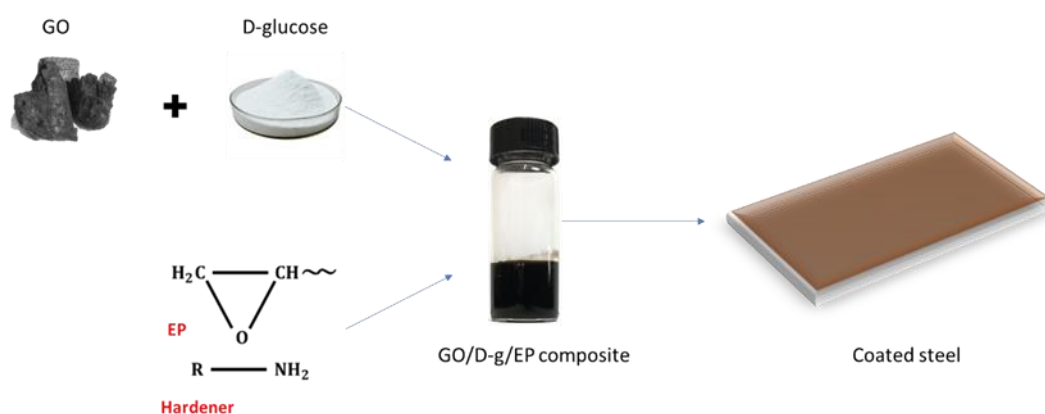


Figure 1. A schematic presentation of m-GO/EP coating.

3. RESULTS AND DISCUSSION

3.1 The Influence of Loading EP

The influence of EP precursor mass loading on charge carrier transfer in modified GO/EP composites is widely acknowledged. Therefore, it becomes crucial to carefully control the amount of EP filling during the fabrication process to enhance the electrochemical properties of these composites. Figure 2 displays the coatings before subjecting them to a corrosion test in a 3.5 wt.% NaCl solution. Additionally, various studies have highlighted the exceptional characteristics of GO.

But when GO is changed into a thick atomic layer with a honeycomb lattice, graphene layers stack on top of each other in a way that cannot be undone. This makes it hard for electrolytes to move around. EP materials are commonly incorporated into the modified GO to overcome this limitation, reduce graphene restacking, and prevent aggregation. So, this work looks at how the mass loading of EP precursors affects the development of modified GO/EP composites and how well they work electrochemically. The researchers controlled EP mass loading by adjusting the weight proportion of GO to EP.

2.5 Coating Preparation

Before coating, the mild steels were cleaned with distilled water and dried. The coatings were generated by combining the appropriate amount of filler (EP, 0.1% m-GO, 0.5% m-GO, and 0.7% m-GO) with EP. Furthermore, bare steel was employed as a blank control group. After being dried, the samples were cured in a 50 °C oven for one hour. Meanwhile, Figure 1 depicts the m-GO/EP coating preparation.

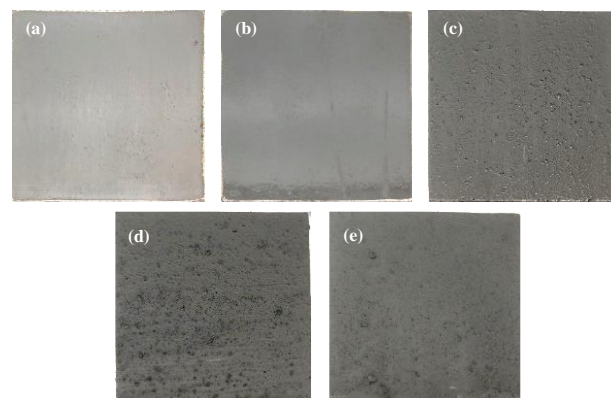


Figure 2. Picture of coatings before immersed in 3.5 wt.% NaCl solution for corrosion test (a) bare steel; (b) EP; (c) 0.1% m-GO/EP; (d) 0.5% m-GO/EP and (e) 0.7% m-GO/EP.

3.2 Polarization Curves

Figure 3 shows polarization potentiodynamic data on how different coatings resist corrosion after being submerged for 42 days in a 3.5 wt% NaCl solution. Table 2 presents essential parameters such as corrosion potential (E_{corr}), corrosion density (I_{corr}), corrosion rate, and polarization resistance for each coating. However, relying solely on the corrosion potential (E_{corr}) to assess the coatings' anticorrosion effectiveness is inadequate, as it mainly describes the materials' thermodynamic properties and doesn't provide a complete picture of their corrosion resistance.

According to earlier studies [40], [41] lower corrosion density (I_{corr}) and lower corrosion rates, in general, indicate superior corrosion protection. The bare steel, EP, 0.1% m-GO/EP, 0.5% m-GO/EP, and 0.7% m-GO/EP coating are $-0.0078196 \text{ A/cm}^2$, $-0.0052484 \text{ A/cm}^2$, -0.007157 A/cm^2 , $-0.0023857 \text{ A/cm}^2$ and -0.00167 A/cm^2 after immersion in 3.5 wt.% NaCl solution for 42 days (Table 2), respectively. Larger E_{corr} values indicate that corrosion requires a stronger driving force. On the other hand, a smaller i_{corr} suggests slower electrical movement. Figure 3 illustrates that while EP coatings have a minimal impact on improving the corrosion protection of mild steel, GO-based coatings significantly enhance corrosion resistance. However, as the quantity of GO in the layers increased, the deterioration rate of EP layers also increased.

The study shows that the anticorrosion effect improves with increasing GO concentration up to a large GO percentage. Beyond this percentage, a high percentage of GO creates a conductive channel from the metal substrate to the coating's outer edge, which can promote metal corrosion. Therefore, the researchers obtained the corrosion rates of different coatings, as presented in Table 2. Adding 0.7% m-GO/EP led to a gradual increase in the corrosion rate (-19.405 mm/year). This result indicates that GO accumulation in the coating caused an increase in coating defects, accelerating the corrosion reaction.

Table 2 Parameters of polarization curves for different coatings after 42 days immersed in 3.5% NaCl solution

Sample	E_{corr} (V _{SCE})	i_{corr} (A/cm ²)	Corrosion rate (mm/year)	Polarization resistance (Ω)
Bare steel	0.82102	-0.0078196	-90.864	-3.3323
EP	0.6996	-0.0052484	-60.986	-4.9648
0.1% m-GO/EP	0.73202	-0.007157	-83.163	-3.6409
0.5% m-GO/EP	0.79173	-0.0023857	-27.721	-10.923
0.7% m-GO/EP	0.73166	-0.00167	-19.405	-15.604

The incorporation of GO into the composite coating led to a significant reduction in the corrosion density (i_{corr}) compared to untreated steel and EP coatings. The i_{corr} values for the 0.1% m-GO/EP, 0.5% m-GO/EP, and 0.7% m-GO/EP coatings were indicating improved corrosion resistance with increasing GO concentration. Notably, the composite coating produced using a 0.7% m-GO nanosheet solution exhibited superior corrosion resistance when immersed in a 3.5 wt.% NaCl solution. The 0.7% m-GO/EP coating demonstrated excellent substrate adhesion and showed significant anticorrosion performance, achieving a high corrosion resistance value of -19.405 mm/year . This result highlights the effectiveness of the 0.7% m-GO/EP coating in protecting against corrosion.

The improved corrosion protection of the m-GO/EP coating can be attributed, in part, to the excellent distribution of GO within the coating. Moreover, the synergistic effect of EP and GO leads to forming a higher-quality composite coating, which enhances the diffusion path of O_2 and H_2O , further contributing to its corrosion resistance. The potentiodynamic polarization curves provided evidence that the corrosion resistance performance of the m-GO/EP coatings predominantly depends on the quantity of embedded GO. In other words, the amount of GO in the composite directly affects the coating's corrosion protection properties.

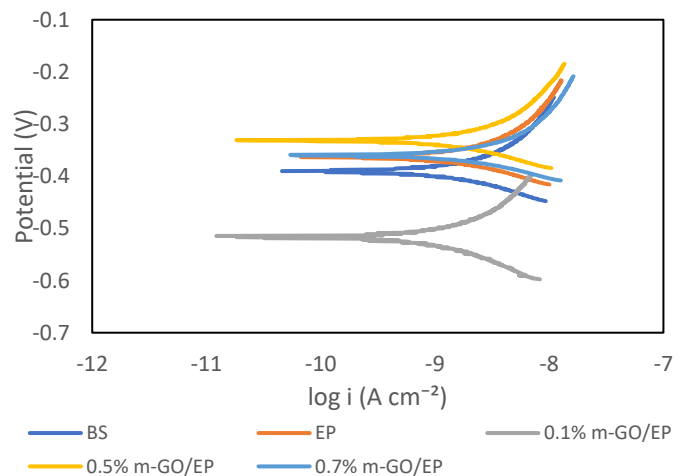


Figure 3. Polarization potentiodynamic curves for bare steel, EP, 0.1% m-GO/EP, 0.5% m-GO/EP, and 0.7% m-GO/EP coated electrode immersed in 3.5% NaCl solution after 42 days.

3.3 Electrical Impedance Spectroscopy (EIS)

The corrosion protection mechanisms of GO-based coatings are complex and involve processes like metal oxide passivation, barrier protection, and anode protection [42], [43]. Incorporating the D-g/GO composite may enhance the EP polymer's anticorrosion mechanism. The cracks and holes in the coating can allow corrosive species such as H_2O and O_2 to penetrate the layer and lead to substrate degradation. However, with the dissemination of the D-g/GO composite in the coating, graphene, and epoxy fill these holes, improving the protective layer.

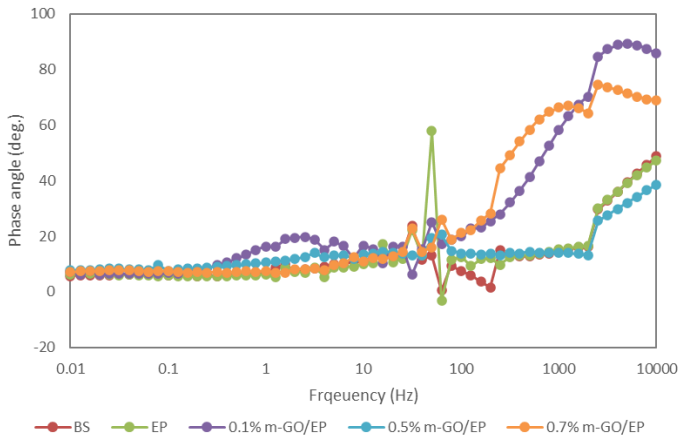


Figure 4. Bode diagrams (phase angle) of coatings immersed in 3.5 wt.% NaCl solution after 42 days.

The phase angle of a perfect coating is close to 90°, while it is close to 0° for an uncoated material [44]. In this study, the high-frequency phase angle of the EP coating was found to be 47.20° (Figure 4), indicating that the integrity of the EP coating is not sufficient. However, the capacitance behavior of the 0.1% m-GO/EP coating exhibited the broadest frequency band, and its phase angle increased by almost 90°, suggesting that the addition of 0.1 mg/mL GO may contribute to a thicker and less defective EP coating. These observations might seem contradictory to the

potentiodynamic polarization curve results. Furthermore, Figure 4.14 indicates that adding 0.7 mg/mL GO led to an increase in temperature of approximately 70°, which may also enhance the corrosion rate. This suggests that a higher concentration of GO in the composite might have adverse effects on the corrosion resistance, despite improving the integrity of the EP coating at a lower concentration.

Figure 5 shows the EIS results for several coatings in a 3.5 wt.% NaCl solution at ambient temperature. The impedance value, represented as |Z|, reflects the overall impedance of the coating and substrate, with its magnitude indicating the level of corrosion protection provided by the specimen. Comparing the different coatings, it is observed that the |Z| value for the 0.7% m-GO/EP coating was significantly lower, indicating that the corrosion resistance of EP coatings is enhanced when modified with GO. In other words, the 0.7% m-GO/EP coating displayed superior corrosion protection compared to the other coatings. Additionally, the phase angle at high frequency can also measure the coating's effectiveness in the presence of a corrosive medium. The phase angle can provide valuable data about the performance of the coating under the impact of corrosive conditions, further supporting the assessment of the coating's corrosion resistance performance.

Table 3 The electrochemical parameters obtained from impedance data of the coatings immersed in 3.5 wt.% NaCl solution for 42 days

Sample	R _p (kΩcm ²)	R _s (kΩcm ²)	CPE _{dl}	
			Y ₀ (Ω ⁻¹ cm ⁻² s ⁿ)	n
Bare steel	3.5114 × 10 ⁶	2.2344 × 10 ⁶	1.4704 × 10 ⁻⁹	0.95876
EP	7.5886 × 10 ⁶	1.2537 × 10 ⁶	8.3615 × 10 ⁻⁹	0.48668
0.1% m-GO/EP	7.6898 × 10 ⁶	-12580	1.6972 × 10 ⁻⁹	0.62967
0.5% m-GO/EP	4.5299 × 10 ⁶	-11990	2.0328 × 10 ⁻⁹	0.80165
0.7% m-GO/EP	40984 × 10 ⁶	1.1347 × 10 ⁶	7.5588 × 10 ⁻¹¹	0.93197

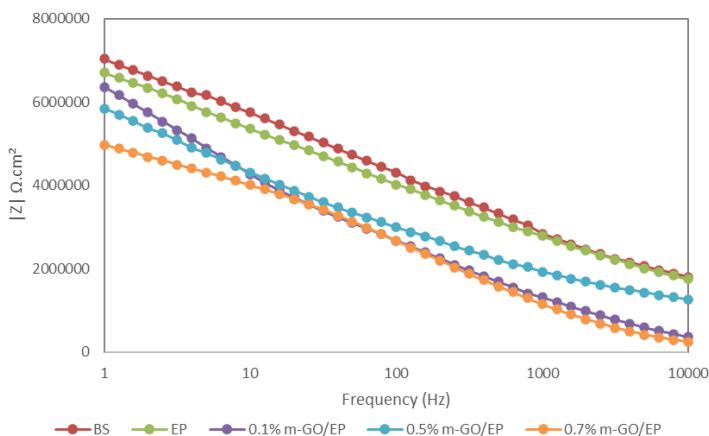


Figure 5. Bode diagrams (impedance modulus) of coatings immersed in 3.5 wt.% NaCl solution after 42 days.

Figure 6 displays Nyquist curves characterized by two-time constant semicircles, which reveal important information about the essential characteristics of the layer and the potential number of localized elements at the metal/coating interface. These curves also represent electrochemical cycles demonstrated by resistance and capacitance elements. The impedance curves are compared with equivalent circuit simulations based on information obtained from two exposure times to analyze these electrochemical aspects of different coatings further. However, the impedance curves may exhibit certain distortions due to the lack of contact uniformity resulting from surface refining and double-layer errors.

The constant phase element (CPE) is introduced into the equivalent circuit simulations to address these issues and compensate for experimental results. The electrode's surface abrasion contributes to the deviations from ideal dielectric behavior, which the CPE helps to account for. By including the CPE in the simulations, researchers can better

assess the electrochemical properties and characteristics of the coatings despite potential experimental limitations.

The electrochemical parameters obtained are brief in Table 3, representing the characteristics of electrolyte resistance (R_p), solution resistance (R_s), and the constant phase element of the double layer (CPE_{dl}). The results show that as the concentration of GO loadings increased in the samples containing 0.1% m-GO/EP, 0.5% m-GO/EP, and 0.7% m-GO/EP, the R_p value decreased. The decreases in R_p for the coated GO samples indicate that these specimens lacked self-healing characteristics in the presence of a coating matrix flaw. In other words, while the incorporation of m-GO improved the corrosion resistance of the epoxy coating by providing a better barrier performance, it could not offer sufficient protection if there was a flaw in the coating.

However, the 0.1% m-GO/EP sample showed a higher R_p than the other coatings. This could be attributed to the effect of modified GO sheets, which reduce the access of corrosive medium through coating pores to the coating/metal interface. The performance of the coating systems with modified GO was better than that of the EP coating alone. Covalent bonds between the modified GO and the EP layer make it harder for corrosive agents to get into the steel substrate. Consequently, harmful electrolyte diffusion is inhibited through coating defects and micropores when a coating is damaged. Modified GO plays a role in restricting the migration of destructive ions into the coating substrate, hence improving the overall corrosion protection performance of the composite coating.

The Nyquist impedance arc provides valuable insights into the resistance and anticorrosion abilities of the coatings. A larger Nyquist impedance arc indicates higher resistance and stronger anticorrosion capabilities. Comparing the EP sample to the other four samples (bare steel, 0.1% m-GO/EP, 0.5% m-GO/EP, and 0.7% m-GO/EP), it is evident that the latter four samples displayed more outstanding capacitive loops. Among them, the 0.1% m-GO/EP sample exhibited the largest loop, indicating excellent anticorrosion properties compared to the other coatings.

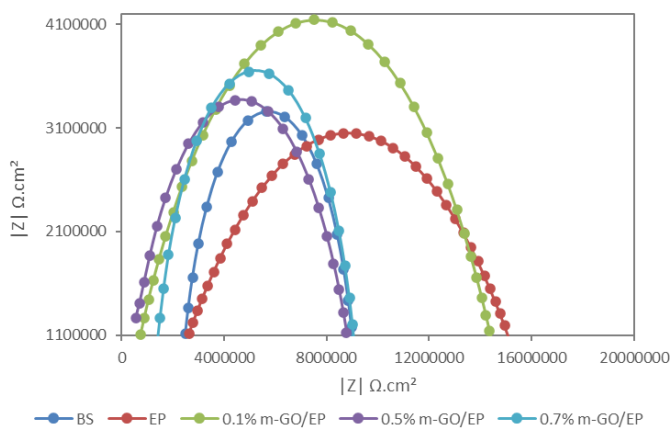


Figure 6. Nyquist curves of coatings immersed in 3.5 wt.% NaCl solution after 42 days.

Figure 6 shows that the 0.1% m-GO/EP coating demonstrated a larger impedance arc, further confirming its superior anticorrosion performance compared to the other coating samples. On the other hand, the diameter of the high-frequency arc for the 0.1% m-GO/EP, 0.5% m-GO/EP, and 0.7% m-GO/EP coatings were much larger than that of the EP sample. This suggests that the modified GO layer coated on the surface improved the performance of the coatings, leading to enhanced corrosion resistance.

The nanostructure of the epoxy composite can play a crucial role in enhancing the adherence and contact between the coating and the substrates. Additionally, adding EP to the steel substrate's surface results in forming an oxide layer that effectively resists corrosion [45]. Incorporating the D-g/GO composite significantly improves the anticorrosion effectiveness of the coatings due to the combined benefits of EP and graphene additions.

In summary, the combination of nanostructured epoxy composite, EP, and graphene (in the form of D-g/GO composite) results in coatings with improved adhesion, strong contacts with substrates, and the ability to form a protective oxide layer on the steel surface, all contributing to enhanced corrosion resistance and protection.

3.4 Surface of Composite Coatings

After removing the coatings, the surfaces of the test samples were immersed in a 3.5 wt.% NaCl solution for 42 days was examined, as shown in Figure 7. The pure EP coating exhibited a rusted surface with damaged microparticles surrounding it, indicating a low anticorrosion performance. In contrast, a wedge of microparticles was observed surrounding the damaged region for the 0.5% m-GO/EP and 0.7% m-GO/EP coatings. This observation aligns with the fact that GO sheets can effectively block the entry of highly corrosive molecules, at least for a limited period.

The 0.7% m-GO/EP coating displayed fewer invisible rusts on the metal substrate than the EP coating. The presence of m-GO/EP on the scratched surface might have physically adsorbed onto the metal surfaces, preventing the entry of corrosive ions and thereby inhibiting corrosion damage of the exposed metal in the presence of graphene.

In short, the microstructure analysis of the coated samples showed that adding m-GO to the EP coating made it better at protecting against corrosion because it could block molecules that cause corrosion and physically protect the metal surfaces from corrosion damage.

The epoxy matrix in the pure EP coating is typically considered a physical protective film that prevents hostile species from penetrating the layer [46]. However, due to the coating's poor barrier quality, corrosive species can quickly enter the layer and accomplish the layer's surface. Consequently, the coating penetrates, and the steel loses its protection based on the polymer matrix. Besides, composite coatings, especially m-GO/EP, demonstrated superior properties. Adding GO sheets in the m-GO/EP coating could improve the dispersion pathway of corrosive molecules, leading to enhanced corrosion protection performance.

However, GO's limited distribution and dispersion seriously diminished the practical application of the physical barrier effect. In summary, while the pure EP coating relies on its epoxy matrix for protection, composite coatings, such as m-GO/EP, offer improved anticorrosion due to the addition of GO sheets. The distribution and dispersion of GO within the coating, however, is what limits its effectiveness.

Indeed, the strong electrical conductivity of GO sheets can have a dual effect on the corrosive response of the metal. On the one hand, it may promote corrosion by facilitating electron transfer and creating an environment conducive to corrosion. On the other hand, the m-GO/EP composite coating demonstrated the highest level of protection among coatings, suggesting that the benefits outweighed the drawbacks. Several explanations can be derived for the excellent anticorrosion performance of m-GO/EP coating. Firstly, the unique granular structure of m-GO sheets provided a physical barrier feature that enhanced the diffusion route of highly corrosive compounds. This improved barrier performance contributed to the long-term protection of the material from corrosive agents.

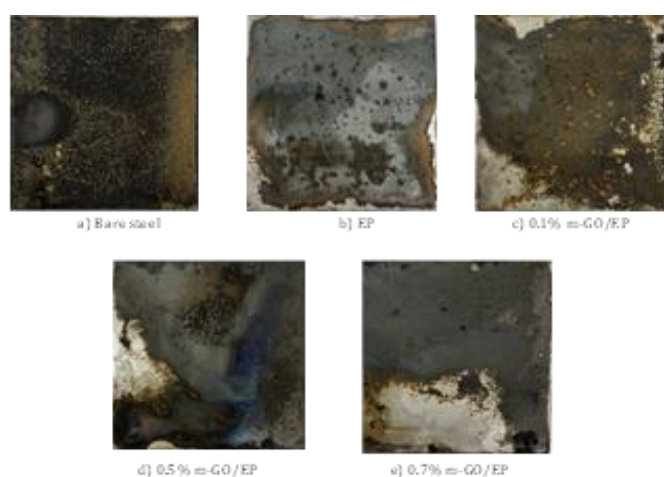


Figure 7. Photograph of coatings immersed in 3.5 wt.% NaCl solution for corrosion test (a) bare steel; (b) EP; (c) 0.1% m-GO/EP; (d) 0.5% m-GO/EP and (e) 0.7% m-GO/EP after 42 days.

Secondly, the poor electrical conductivity of m-GO played a significant role in inhibiting steel corrosion. By limiting electron transfer and hindering corrosion, m-GO helped protect the steel substrate from deterioration. Lastly, the presence of D-g molecules further enhanced the interaction between the D-g/GO and epoxy medium, leading to improved durability of the epoxy coating. This synergy endowed the m-GO/EP composite coating with robust anticorrosion capabilities, making it a practical choice for corrosion protection applications.

The electrochemical experimental data demonstrates that incorporating GO and EP significantly enhances the coating's anticorrosion capability. This improvement is attributed to various factors, including an improved hydrophobic property, a sustained path for corrosive medium, crosslinking of D-g on the GO surface aiding in passivation film formation, and homogeneous distribution of m-GO/EP, effectively clogging coating flaws and

preventing corrosive material from reaching the metal substrate. Additionally, the presence of EP particles enhances the adherence of the composite coating to the metal substrate, ensuring long-term anticorrosion by providing stable protection. The combined effect of GO and EP in the coating results in a highly effective and secure anticorrosion solution.

4. CONCLUSION

In this study, GO was successfully modified with D-g using an in-situ chemical modification method, resulting in 0.7% m-GO/EP coating with excellent anticorrosion properties, even in highly corrosive environments. Earlier research has extensively investigated the impact of surface-functionalized GO particles on the corrosion resistance of polymeric coatings. However, the technique may not effectively prevent corrosion when the coating is damaged or flawed. A novel approach was exploited to adopt this by varying GO sheets with EP, creating a combination of GO sheets' barrier effect and m-GO/EP's inhibitory activity. The m-GO/EP particles are less hazardous than conventional active pigments like GO but possess comparable inhibitory activity and more potent barrier properties. This approach opens potential applications in forming a single barrier layer that combines inhibitory and barrier effects in typical multilayer anticorrosion coatings.

ACKNOWLEDGMENTS

This research work was financially supported by Fundamental Research Grant Scheme FRGS/1/2020/TK0/UM/02/8 (FP023-2020).

REFERENCES

- [1] H. M. Abd El-Lateef, "Corrosion inhibition characteristics of a novel salicylidene isatin hydrazine sodium sulfonate on carbon steel in HCl and a synergistic nickel ions additive: A combined experimental and theoretical perspective," *Appl Surf Sci*, vol. 501, Jan. 2020, doi: 10.1016/j.apsusc.2019.144237.
- [2] E. B. Caldona, D. W. Smith, and D. O. Wipf, "Protective action of semi-fluorinated perfluorocyclobutyl polymer coatings against corrosion of mild steel," *J Mater Sci*, vol. 55, no. 4, pp. 1796–1812, Feb. 2020, doi: 10.1007/s10853-019-04025-2.
- [3] S. A. Umoren, M. M. Solomon, A. Madhankumar, and I. B. Obot, "Exploration of natural polymers for use as green corrosion inhibitors for AZ31 magnesium alloy in saline environment," *Carbohydr Polym*, vol. 230, Feb. 2020, doi: 10.1016/j.carbpol.2019.115466.
- [4] Y. Jing, P. Wang, Q. Yang, Q. Wang, and Y. Bai, "MoS₂ decorated with ZrO₂ nanoparticles through mussel-inspired chemistry of dopamine for reinforcing anticorrosion of epoxy coatings," *Colloids Surf A Physicochem Eng Asp*, vol. 608, Jan. 2021, doi: 10.1016/j.colsurfa.2020.125625.

- [5] C. Wang, Z. Li, H. Zhao, G. Zhang, T. Ren, and Y. Zhang, "Enhanced anticorrosion and antiwear properties of Ti-6Al-4V alloys with laser texture and graphene oxide coatings," *Tribol Int*, vol. 152, Dec. 2020, doi: 10.1016/j.triboint.2020.106475.
- [6] H. Cen and Z. Chen, "Amide functionalized graphene oxide as novel and effective corrosion inhibitor of carbon steel in CO₂-saturated NaCl solution," *Colloids Surf A Physicochem Eng Asp*, vol. 615, Apr. 2021, doi: 10.1016/j.colsurfa.2021.126216.
- [7] Z. T. Khodair, A. A. Khadom, and H. A. Jasim, "Corrosion protection of mild steel in different aqueous media via epoxy/nanomaterial coating: Preparation, characterization and mathematical views," *Journal of Materials Research and Technology*, vol. 8, no. 1, pp. 424-435, Jan. 2019, doi: 10.1016/j.jmrt.2018.03.003.
- [8] Y. Zhang, F. Chen, Y. Zhang, and C. Du, "Influence of graphene oxide additive on the tribological and electrochemical corrosion properties of a PEO coating prepared on AZ31 magnesium alloy," *Tribol Int*, vol. 146, Jun. 2020, doi: 10.1016/j.triboint.2019.106135.
- [9] Y. Wang, S. Lim, J. L. Luo, and Z. H. Xu, "Tribological and corrosion behaviors of Al₂O₃/polymer nanocomposite coatings," *Wear*, vol. 260, no. 9-10, pp. 976-983, May 2006, doi: 10.1016/j.wear.2005.06.013.
- [10] J. R. Xavier, "Electrochemical and Mechanical Investigation of Newly Synthesized NiO-ZrO₂ Nanoparticle-Grafted Polyurethane Nanocomposite Coating on Mild Steel in Chloride Media," *J Mater Eng Perform*, vol. 30, no. 2, pp. 1554-1566, Feb. 2021, doi: 10.1007/s11665-020-05448-8.
- [11] C. X. Wang and X. F. Zhang, "A non-particle and fluorine-free superhydrophobic surface based on one-step electrodeposition of dodecyltrimethoxysilane on mild steel for corrosion protection," *Corros Sci*, vol. 163, Feb. 2020, doi: 10.1016/j.corsci.2019.108284.
- [12] J. R. Xavier, "Electrochemical and dynamic mechanical studies of newly synthesized polyurethane/SiO₂-Al₂O₃ mixed oxide nanocomposite coated steel immersed in 3.5% NaCl solution," *Surfaces and Interfaces*, vol. 22, Feb. 2021, doi: 10.1016/j.surfin.2020.100848.
- [13] Z. Zhou, X. Ji, S. Pourhashem, J. Duan, and B. Hou, "Investigating the effects of g-C₃N₄/Graphene oxide nanohybrids on corrosion resistance of waterborne epoxy coatings," *Compos Part A Appl Sci Manuf*, vol. 149, Oct. 2021, doi: 10.1016/j.compositesa.2021.106568.
- [14] S. P. Vinodhini and J. R. Xavier, "Evaluation of corrosion protection performance and mechanical properties of epoxy-triazole/graphene oxide nanocomposite coatings on mild steel," *J Mater Sci*, vol. 56, no. 11, pp. 7094-7110, Apr. 2021, doi: 10.1007/s10853-020-05636-w.
- [15] W. Brostow, M. Dutta, and P. Rusek, "Modified epoxy coatings on mild steel: Tribology and surface energy," *Eur Polym J*, vol. 46, no. 11, pp. 2181-2189, Nov. 2010, doi: 10.1016/j.eurpolymj.2010.08.006.
- [16] J. R. Beryl and J. R. Xavier, "A study on the anticorrosion performance of epoxy nanocomposite coatings containing epoxy-silane treated nanoclay on mild steel in chloride environment," *Journal of Polymer Research*, vol. 28, no. 5, May 2021, doi: 10.1007/s10965-021-02512-2.
- [17] G. Jena, R. P. George, and J. Philip, "Fabrication of a robust graphene oxide-nano SiO₂-polydimethylsiloxane composite coating on carbon steel for marine applications," *Prog Org Coat*, vol. 161, Dec. 2021, doi: 10.1016/j.porgcoat.2021.106462.
- [18] G. Xue et al., "A facile approach to synthesize in situ functionalized graphene oxide/epoxy resin nanocomposites: mechanical and thermal properties," *J Mater Sci*, vol. 54, no. 22, pp. 13973-13989, Nov. 2019, doi: 10.1007/s10853-019-03901-1.
- [19] X. Wang, F. Tang, X. Qi, Z. Lin, D. Battocchi, and X. Chen, "Enhanced protective coatings based on nanoparticle fullerene c₆₀ for oil & gas pipeline corrosion mitigation," *Nanomaterials*, vol. 9, no. 10, Oct. 2019, doi: 10.3390/nano9101476.
- [20] A. A. P. O. Amorim, M. G. Oliveira, M. C. Mancini, and A. S. Sirqueira, "Rheological, EMI and corrosion properties of epoxy coating with nanoparticle and conductive carbon black," *SN Appl Sci*, vol. 3, no. 2, Feb. 2021, doi: 10.1007/s42452-021-04247-7.
- [21] B. Ramezanzadeh, E. Ghasemi, M. Mahdavian, E. Changizi, and M. H. Mohamadzadeh Moghadam, "Covalently-grafted graphene oxide nanosheets to improve barrier and corrosion protection properties of polyurethane coatings," *Carbon N Y*, vol. 93, pp. 555-573, Aug. 2015, doi: 10.1016/j.carbon.2015.05.094.
- [22] A. A. Javidparvar, R. Naderi, and B. Ramezanzadeh, "Designing a potent anti-corrosion system based on graphene oxide nanosheets non-covalently modified with cerium/benzimidazole for selective delivery of corrosion inhibitors on steel in NaCl media," *J Mol Liq*, vol. 284, pp. 415-430, Jun. 2019, doi: 10.1016/j.molliq.2019.04.028.
- [23] M. Mo et al., "Excellent tribological and anti-corrosion performance of polyurethane composite coatings reinforced with functionalized graphene and graphene oxide nanosheets," *RSC Adv*, vol. 5, no. 70, pp. 56486-56497, 2015, doi: 10.1039/c5ra10494g.
- [24] S. S. Ashok Sharma, S. Bashir, R. Kasi, and R. T. Subramaniam, "The significance of graphene based composite hydrogels as smart materials: A review on the fabrication, properties, and its applications," *FlatChem*, vol. 33, Elsevier B.V., May 01, 2022. doi: 10.1016/j.flatc.2022.100352.
- [25] A. K. Geim and K. S. Novoselov, "The rise of graphene," 2009. [Online]. Available: www.nature.com/naturematerials
- [26] F. Chen, J. Ying, Y. Wang, S. Du, Z. Liu, and Q. Huang, "Effects of graphene content on the microstructure and properties of copper matrix composites," *Carbon N Y*, vol. 96, pp. 836-842, Jan. 2016, doi: 10.1016/j.carbon.2015.10.023.
- [27] O. Tapasztó et al., "High orientation degree of graphene nanoplatelets in silicon nitride composites prepared by spark plasma sintering," *Ceram Int*, vol.

- 42, no. 1, pp. 1002–1006, 2016, doi: 10.1016/j.ceramint.2015.09.009.
- [28] R. Atif, I. Shyha, and F. Inam, “Mechanical, thermal, and electrical properties of graphene-epoxy nanocomposites-A review,” *Polymers*, vol. 8, no. 8. MDPI AG, Aug. 04, 2016. doi: 10.3390/polym8080281.
- [29] D. G. Papageorgiou, I. A. Kinloch, and R. J. Young, “Mechanical properties of graphene and graphene-based nanocomposites,” *Progress in Materials Science*, vol. 90. Elsevier Ltd, pp. 75–127, Oct. 01, 2017. doi: 10.1016/j.pmatsci.2017.07.004.
- [30] M. Calovi, S. Rossi, F. Deflorian, S. Dirè, and R. Ceccato, “Graphene-based reinforcing filler for double-layer acrylic coatings,” *Materials*, vol. 13, no. 20, pp. 1–27, Oct. 2020, doi: 10.3390/ma13204499.
- [31] S. C. Ray, “Application and Uses of Graphene Oxide and Reduced Graphene Oxide,” in *Applications of Graphene and Graphene-Oxide Based Nanomaterials*, Elsevier, 2015, pp. 39–55. doi: 10.1016/b978-0-323-37521-4.00002-9.
- [32] M. Calovi, S. Rossi, F. Deflorian, S. Dirè, and R. Ceccato, “Effect of functionalized graphene oxide concentration on the corrosion resistance properties provided by cathodic acrylic coatings,” *Mater Chem Phys*, vol. 239, Jan. 2020, doi: 10.1016/j.matchemphys.2019.121984.
- [33] S. Y. Yang et al., “Synergetic effects of graphene platelets and carbon nanotubes on the mechanical and thermal properties of epoxy composites,” *Carbon N Y*, vol. 49, no. 3, pp. 793–803, Mar. 2011, doi: 10.1016/j.carbon.2010.10.014.
- [34] X. Wang, W. Xing, P. Zhang, L. Song, H. Yang, and Y. Hu, “Covalent functionalization of graphene with organosilane and its use as a reinforcement in epoxy composites,” *Compos Sci Technol*, vol. 72, no. 6, pp. 737–743, Mar. 2012, doi: 10.1016/j.compscitech.2012.01.027.
- [35] A. Yadav, R. Kumar, and B. Sahoo, “Graphene Oxide Coatings on Amino Acid Modified Fe Surfaces for Corrosion Inhibition,” *ACS Appl Nano Mater*, vol. 3, no. 4, pp. 3540–3557, Apr. 2020, doi: 10.1021/acsanm.0c00243.
- [36] A. Yadav, R. Kumar, H. K. Choudhary, and B. Sahoo, “Graphene-oxide coating for corrosion protection of iron particles in saline water,” *Carbon N Y*, vol. 140, pp. 477–487, Dec. 2018, doi: 10.1016/j.carbon.2018.08.062.
- [37] A. Yadav, R. Kumar, U. P. Pandey, and B. Sahoo, “Role of oxygen functionalities of GO in corrosion protection of metallic Fe,” *Carbon N Y*, vol. 173, pp. 350–363, Mar. 2021, doi: 10.1016/j.carbon.2020.11.029.
- [38] M. Cui, S. Ren, H. Zhao, Q. Xue, and L. Wang, “Polydopamine coated graphene oxide for anticorrosive reinforcement of water-borne epoxy coating,” *Chemical Engineering Journal*, vol. 335, pp. 255–266, Mar. 2018, doi: 10.1016/j.cej.2017.10.172.
- [39] P. Bansal, A. S. Panwar, and D. Bahadur, “Molecular-Level Insights into the Stability of Aqueous Graphene Oxide Dispersions,” *Journal of Physical Chemistry C*, vol. 121, no. 18, pp. 9847–9859, May 2017, doi: 10.1021/acs.jpcc.7b00464.
- [40] X. R. Liu, X. X. Sheng, X. Y. Yuan, J. K. Liu, X. W. Sun, and X. H. Yang, “Research on correlation between corrosion resistance and photocatalytic activity of molybdenum zinc oxide modified by carbon quantum dots pigments,” *Dyes and Pigments*, vol. 175, Apr. 2020, doi: 10.1016/j.dyepig.2019.108148.
- [41] Y. Guo et al., “Corrosion resistance and biocompatibility of graphene oxide coating on the surface of the additively manufactured NiTi alloy,” *Prog Org Coat*, vol. 164, Mar. 2022, doi: 10.1016/j.porgcoat.2022.106722.
- [42] Y. Jafari, S. M. Ghoreishi, and M. Shabani-Nooshabadi, “Polyaniline/Graphene nanocomposite coatings on copper: Electropolymerization, characterization, and evaluation of corrosion protection performance,” *Synth Met*, vol. 217, pp. 220–230, Jul. 2016, doi: 10.1016/j.synthmet.2016.04.001.
- [43] Z. Tian et al., “Recent progress in the preparation of polyaniline nanostructures and their applications in anticorrosive coatings,” *RSC Advances*, vol. 4, no. 54. Royal Society of Chemistry, pp. 28195–28208, 2014. doi: 10.1039/c4ra03146f.
- [44] B. Ramezanzadeh, E. Ghasemi, M. Mahdavian, E. Changizi, and M. H. M. Moghadam, “Covalently-grafted graphene oxide nanosheets to improve barrier and corrosion protection properties of polyurethane coatings,” 2015, doi: 10.1016/j.carbon.2015.05.094.
- [45] P. Wang and D. Cai, “Preparation of Graphene-Modified Anticorrosion Coating and Study on Its Corrosion Resistance Mechanism,” *International Journal of Photoenergy*, vol. 2020, 2020, doi: 10.1155/2020/8846644.
- [46] A. A. Javidparvar, R. Naderi, and B. Ramezanzadeh, “Epoxy-polyamide nanocomposite coating with graphene oxide as cerium nanocontainer generating effective dual active/barrier corrosion protection,” *Compos B Eng*, vol. 172, no. January, pp. 363–375, 2019, doi: 10.1016/j.compositesb.2019.05.055.